

Up-regulation of MiR-146b-5p Inhibits Fibrotic Lung Pericytes via Inactivation of the Notch1/PDGFR β /ROCK1 Pathway

(lung fibrosis / miR-146b-5p / Notch1/PDGFR β /ROCK1 / extracellular matrix / bleomycin)

W. SHUAI¹, Q. CHEN², X. ZHOU¹

¹Departments of Critical Care Medicine, Hunan Provincial People's Hospital (The First Affiliated Hospital of Hunan Normal University), Changsha 410005, Hunan, China

²Department of Nephrology, Shanghai General Hospital, Shanghai 200000, China

Abstract. Lung fibrosis is a serious human pathology. MiR-146b-5p is down-regulated in idiopathic pulmonary fibrosis, and the Notch1/PDGFR β /ROCK1 pathway is activated. However, the relation between miR-146b-5p and the Notch1/PDGFR β /ROCK1 pathway in lung fibrosis remains unclear. To investigate the function of miR-146b-5p in lung fibrosis, an *in vivo* model of lung fibrosis was established in mice by bleomycin. The fibrosis in lung tissues of mice was observed by HE, Masson and Sirius Red staining. Lung pericytes were isolated and identified by fluorescence microscopy. Immunofluorescence staining and Western blot were used to investigate the expression of desmin, NG2, collagen I and α -SMA. CCK8

assay was used to assess the cell viability, and flow cytometry was performed to evaluate the cell cycle in pericytes. Furthermore, the correlation between miR-146b-5p and Notch1 was analysed by Spearman analysis. The mechanism by which miR-146b-5p affects pericytes and lung fibrosis via the Notch1/PDGFR β /ROCK1 pathway was explored by RT-qPCR, Western blot, immunofluorescence staining and dual luciferase reporter gene assay. In bleomycin-treated mice, miR-146b-5p was down-regulated, while Notch1 was up-regulated. Up-regulation of miR-146b-5p significantly inhibited the viability and induced G1 phase arrest of lung pericytes. MiR-146b-5p mimics up-regulated miR-146b-5p, desmin, and NG2 and down-regulated α -SMA and collagen I in the lung pericytes. Additionally, miR-146b-5p was negatively correlated with Notch1, and miR-146b-5p interacted with Notch1. Over-expression of miR-146b-5p inactivated the Notch1/PDGFR β /ROCK1 pathway. Our results indicate that up-regulation of miR-146b-5p inhibits fibrosis in lung pericytes via modulation of the Notch1/PDGFR β /ROCK1 pathway. Thus, our study might provide a novel target against lung fibrosis.

Received September 1, 2022. Accepted March 2, 2023.

This study was supported by the Hunan Clinical Medical Technology Innovation Guidance Project (2020SK50924).

Corresponding author: Xu Zhou, Departments of Critical Care Medicine, Hunan Provincial People's Hospital (The First Affiliated Hospital of Hunan Normal University), Jiefang West Road, No. 61, Changsha 410005, Hunan, China. Phone: (+86) 139 0731 9339; e-mail: zhouxu66882022@163.com

Abbreviations: α -SMA – alpha-smooth muscle actin, CCK8 – cell counting kit 8, DAPI – 4',6-diamidino-2-phenylindole, DMEM – Dulbecco's modified Eagle's medium, ECM – extracellular matrix, EDTA – ethylene diamine tetraacetic acid, EMT – epithelial-mesenchymal transition, FBS – foetal bovine serum, HE staining – haematoxylin and eosin staining, HIF-1 α – hypoxia-inducible factor 1 alpha, IHC – immunohistochemistry, IPF – idiopathic pulmonary fibrosis, MUT – mutated type, NG2 – neural/glial antigen 2, PAGE – polyacrylamide gel electrophoresis, PDGFR β – platelet-derived growth factor receptor beta, PI3K – phosphoinositide 3-kinase, PLC – phospholipase C, Ras – rat sarcoma, ROCK1 – Rho-associated coiled-coil containing protein kinase 1, RT-qPCR – reverse transcription quantitative PCR, SD – standard deviation, SDS-PVDF – sodium dodecyl sulphate polyvinylidene difluoride, Twist1 – Twist-related protein 1, UTR – untranslated region, WT – wild type, YAP1 – yes-associated protein 1.

Introduction

Lung fibrosis is a chronic and progressive scarring lung disease categorized under idiopathic interstitial pneumonia (Chanda et al., 2019; Joannes et al., 2022). Meanwhile, it has been reported that excessive proliferation of pericytes could lead to the development of lung fibrosis (Hung et al., 2019; Affandi et al., 2022). At present, drug administration is the major treatment against lung fibrosis; however, the outcomes remain limited (Maher and Streck, 2019; Karman et al., 2021). Therefore, it is urgent to discover new strategies against lung fibrosis.

It has been reported that Notch1/PDGFR β /ROCK1 signalling was activated during the progression of lung fibrosis, and this signalling pathway might promote the

development of lung fibrosis via mediating the proliferation and differentiation of lung pericytes (Wang et al., 2019). It is known that exosomal miR-107 produced by pulmonary vascular endothelial cells may alleviate pericyte-induced fibrosis by inhibiting signalling pathways including HIF-1 α /Notch1/PDGFR β /YAP1/Twist1 (Wang et al., 2021), and regulation of the Notch1 pathway might be a promising therapeutic strategy against lung fibrosis. Meanwhile, endostatin-modified polypeptide (PEP06) could inhibit EMT process by modulation of miR-146b-5p, thus attenuating cancer growth and metastasis (Yu et al., 2018). MiR-146b-5p is known to be abnormally down-regulated in idiopathic pulmonary fibrosis (IPF) patient fibroblasts, and this phenomenon could contribute to the fibrosis and up-regulation of ECM-related mRNAs (Mullenbrock et al., 2018). Moreover, miR-146b-5p was involved in alveolar and myocardial hypoxia-induced cardiac fibrosis, which can cause the occurrence of heart failure (Chouvarine et al., 2019). In this study, a bioinformatic tool predicted that miR-146b-5p could target Notch1. However, the mechanism underlying the function of miR-146b-5p in the lung fibrosis remains unclear.

Based on the above backgrounds, this study aimed to investigate the relation between miR-146b-5p and Notch1 in lung fibrosis. We hope this research can provide a theoretical basis for exploring new strategies against lung fibrosis.

Material and Methods

In vivo model of lung fibrosis

Male mice (BALB/c, N = 5 per group, Chinese Academy of Sciences, Shanghai, China) were randomly divided into two groups (control and model). For constructing an *in vivo* model of lung fibrosis, mice in the model group were anesthetized by injecting 10 % chloral hydrate (3 ml/kg body weight) into the abdominal cavity. A middle incision was made in the neck skin to expose the trachea, into which 0.2 ml of bleomycin (5 mg/kg, Sigma-Aldrich, St. Louis, MO) was applied. Physiological saline was used in parallel as a negative control, which was injected into control mice in the same volume. Mice were then placed in a vertical position and rotated to distribute the drug evenly. Mice were sacrificed at 7, 14 and 21 days after injection. Half of the lung tissue was fixed with formaldehyde for paraffin embedding and further staining. The other half of the lung tissue was kept in liquid nitrogen for further use. All procedures were in line with those previously described (Wang et al., 2016).

Haematoxylin and eosin (HE) staining

The paraffin-embedded mouse lung tissues were sectioned to 5 μ m. HE staining was carried out following the kit instructions (Servicebio, Wuhan, China). The paraffin sections were deparaffinized to water. Then, HE staining was successively performed. The sections

were stained with haematoxylin for 5 min and rinsed by tap water, followed by being differentiated by differentiation solution for 3 s. After being rinsed by tap water, the sections were left to return to blue for about 3 s, rinsed by tap water and dehydrated by 85 and 95 % ethanol in turn for 4 min. Afterwards, the sections were stained by eosin dye solution for 5 min and dehydrated three times (5 min each time) with anhydrous ethanol and made transparent by xylene twice for 2 min. Then, the sections were mounted with neutral gum. Finally, the results were observed under a light microscope.

Masson and Sirius Red staining

The lung tissues were fixed in 4 % paraformaldehyde and cut into three thick slices from apex to base along the long axis using a tissue slicer. After embedding in paraffin and sectioning at 4 μ m, samples were stained with Masson and Sirius Red, respectively. Finally, the results were observed under a light microscope.

Immunohistochemistry (IHC) staining

Paraformaldehyde (4 %) was applied to prefix the tissues for 10 min. Subsequently, pre-cooled methanol was applied to fix the samples for 10 min. Primary antibody was applied to incubate the samples at 4 °C overnight: anti-Notch1 (Proteintech, Rosemont, IL; 20687-1-AP, 1 : 50). Goat anti-rabbit IgG antibody (Proteintech; SA00013-2, 1 : 100) was regarded as the secondary antibody. The sample was visualized under a fluorescence microscope (Olympus CX23, Tokyo, Japan).

Cell isolation and culture

The lung tissues of mice with lung fibrosis were harvested and incubated in Dulbecco's modified Eagle's medium (DMEM) with protease and DNase for 30 min at 37 °C. After digestion, tissue lysates were filtered through a 40 μ m filter, centrifuged, and resuspended in cold PBS buffer containing 2 nM EDTA. To isolate pericytes, cells were incubated with anti-PDGFR β polyclonal antibody (#3169, Cell Signaling Technology, Danvers, MA). After washing, cells were incubated in goat anti-IgG microbeads and selected by MACS magnetic separation (Miltenyi Biotec, Bergisch Gladbach, Germany). Selected cells were maintained in DMEM/F12 (Gibco, Waltham, MA) medium supplemented with 10 % foetal bovine serum (FBS) (HyClone, Logan, UT) and 1 % penicillin/streptomycin. The procedure was done in accordance with the previous reference (Wang et al., 2019).

Pericyte identification

Purified pericytes were identified using immunofluorescence staining. Briefly, cells were cultured on coverslips and fixed in 4 % paraformaldehyde. Cells were treated with 0.1 % Triton X-100 to increase membrane permeability. After blocking by incubation for 1 hour in 3 % normal goat serum (Invitrogen, Waltham, MA), cells were incubated with anti-PDGFR- β (#3169, 1 : 100, Cell Signaling Technology), anti-NG2 (SC-20162,

1 : 100, Santa Cruz Biotechnology, Dallas, TX), anti-CD13 (ab108382, 1 : 200, Abcam, Cambridge, UK) or anti- α -SMA (ab5694, 1 : 100, Abcam). The next day, pericytes were incubated with fluorescent secondary antibodies (1 : 200, Invitrogen) for 2 hours at room temperature. DAPI was applied to stain the nuclei for 15 min. Images were taken with a fluorescence microscope (Zeiss, Jena, Germany). Cells were identified in accordance with the previous report (Wang et al., 2019).

Cell transfection

Pericytes (3×10^5 cells/well) were cultured. When the cells reached 70 % confluence, they were transfected with a negative control (NC mimics) and miR-146b-5p mimics (Genepharma, Suzhou, China) for 48 h using Lipofectamine 2000 (Invitrogen) in line with the protocol of the manufacturer.

RT-qPCR

TRIzol (TaKaRa, Kusatsu, Japan) was applied to extract the total RNA in line with the manufacturer's protocol. PrimeScript Kit (CW BIO, Beijing, China) or miRNA 1st Strand cDNA Synthesis Kit (CW BIO) was applied to synthesize the cDNA in accordance with the manufacturer's protocol. The ABI7500 system was applied in real-time quantitative PCR (RT-qPCR) analysis using SYBR Green. RT-qPCR was done three times according to the following protocol: 94 °C for 2 min, followed by 35 cycles (94 °C for 30 s and 55 °C for 45 s). The $2^{-\Delta\Delta CT}$ method was applied for data quantification. β -Actin and U6 were applied for normalization. The primers were obtained from GenePharma (Suzhou, China). MiR-146b-5p: forward, 5'-TGAGAACTGAATCCATAGGCT-3' and reverse 5'-GCTGTCAACGATACGC-TACGTA-3'. U6: forward, 5'-CTCGCTTCGGCAGCA-CA-3' and reverse 5'-AACGCTTCACGAATTTGCGT-3'. α -SMA: forward, 5'-GCCCCCTGAAGAGCATCCGAC-3' and reverse 5'-CCAGAGTCCAGCACAAATACCAGT-3'. Notch1: forward, 5'-TGTGGCTTCTTCTACTGCG-3' and reverse 5'-CTTTGCCGTTGACAGGGTTG-3'. ROCK1: forward, 5'-TGAAAGCCGCACTGATGGAT-3' and reverse 5'-TGCCATCTATTCATTCCAGCCA-3'. PDGFR- β : forward, 5'-TACCCAGCCACTTGAACCTG-3' and reverse 5'-TGTCTGCGTATTTGATGTCTCC-3'. Desmin: forward, 5'-AGAAGCCGATCCAGGCAAAA-3' and reverse 5'-AGGATTACAGGCAGCACACC-3'. Collagen I: forward, 5'-CGACCTCAAGATGTGCCACT-3' and reverse 5'-CCATCGGTCATGCTCTCTCC-3'. NG2: forward, 5'-TAGGGAGCAGGCAAACGAAG-3' and reverse 5'-AAACTCAAACGACGCACAGC-3'. U6: forward, 5'-CTCGCTTCGGCAGCAC-3' and reverse 5'-AACGCTTCACGAATTTGCGT-3'. β -Actin: forward, 5'-ACATCCGTAAAGACCTCTATGCC-3' and reverse 5'-TACTCCTGCTTGCTGATCCAC-3'.

Western blotting

RIPA (Beyotime, Jiangsu, China) was applied to extract the total protein. A bicinchonic acid assay (BCA) kit (Beyotime) was applied for protein quantification.

SDS-PAGE (10 %) was applied to separate the proteins (40 μ g per lane). Subsequently, proteins were transferred to PVDF membranes (Invitrogen). Primary antibodies were applied to incubate the membranes overnight: anti-desmin (Proteintech, Rosemont, IL; 60226-1-Ig, 1 : 500), anti-NG2 (Abcam; ab50009, 1 : 1000), anti- α -SMA (MERCCK, Rahway, NJ; BM0002, 1 : 1000), anti-collagen I (Abcam; ab138492, 1 : 1000), anti-Notch1 (Proteintech; 20687-1-AP, 1 : 1000), anti-PDGFR (Abcam; ab69506, 1 : 1000), anti-ROCK1 (Abcam; ab45171, 1 : 2000) and anti- β -actin (Proteintech; 66009-1-Ig, 1 : 5000) after 5 % skim milk was applied to block the membranes for 1 h. After that, secondary antibodies (HRP-conjugated, Proteintech; SA00001-1, 1 : 5000) were applied to incubate the membranes for 1 h. The ECL kit (Thermo Fisher Scientific, Waltham, MA) was applied to analyse the protein bands. β -Actin was applied for data quantification.

CCK8 assay

Pericytes (5×10^3 per well) were seeded overnight. Afterwards, cells were transfected with NC mimics or miR-146b-5p mimics for 24 h. CCK-8 (10 μ l, Dojindo laboratories, Kumamoto, Japan) was added to the cells at 37 °C for 2 h. Finally, a microplate reader (Bio-Tek, Winooski, VE) was applied to assess the absorbance (450 nm).

Cell cycle detection

Pericytes were treated with NC mimics or miR-146b-5p mimics for 48 h. Then, cell cycle detection was performed using a Cycletest Plus DNA Reagent Kit (BD, Franklin Lakes, NJ). Cells were harvested by accutase treatment and counted with a haemocytometer. Cells (5×10^5) were fixed, permeabilized, and stained in accordance with the manufacturers' instructions. Then, the cells were transferred to a flow cytometry tube and detected by a flow cytometer (A00-1-1102, Beckman Coulter, Brea, CA) with an excitation wavelength of 488 nm and an emission wavelength of 630 nm. The data were analysed using ModFit and FlowJo software by calculating the percentages of cells in cell cycle distribution (G1, S, and G2 to M phases).

Luciferase reporter gene assay

MiR-146b-5p-targeted gene prediction was performed using TargetScan. The results were selected for further analysis. Then, the wild-type (WT) or mutated type (MUT) of Notch1 3'-UTR was built based on the pHG vector (Promega, Madison, WI) and named as WT-Notch1 or MUT-Notch1. Cells were co-transfected with miR-146b-5p mimics, NC mimics and WT- or MUT-Notch1 using Lipofectamine 2000. After 48 h of transfection, luciferase activity was measured using the dual-luciferase reporter assay system (Promega).

Statistical analysis

Three independent experiments were applied in each group, and mean \pm standard deviation (SD) was applied

to express the data. Student's *t*-test (GraphPad Prism7) was applied to analyse the changes. The relation between miR-146b-5p and Notch1 was investigated by Spearman correlation analysis. $P < 0.05$ suggested a significant difference.

Results

An in vivo model of lung fibrosis was successfully established

To detect the function of miR-146b-5p in lung fibrosis, an *in vivo* model of lung fibrosis was constructed. As shown in Fig. 1A, more obvious inflammatory infiltration and fibrosis were shown in the model group compared with control mice. In addition, the expression of Notch1 was significantly higher in mice with lung fibrosis compared with that in the control (Fig. 1B). In contrast, the level of miR-146b-5p in mice with lung fibrosis was much lower than that in the control group

(Fig. 1B). Meanwhile, the miR-146b-5p level was negatively correlated with Notch1 (Fig. 1C). Notch1, collagen I and α -SMA levels were significantly up-regulated in the model group, while the expression of desmin and NG2 was notably down-regulated in mice with the lung fibrosis (Fig. 1D and 1E). In summary, an *in vivo* model of lung fibrosis was successfully established.

Notch1 was identified to be the downstream mRNA of miR-146b-5p

To explore the downstream target of miR-146b-5p, TargetScan was used. As indicated in Fig. 2A, Notch1 was predicted to be the downstream mRNA of miR-146b-5p. In addition, the relative luciferase activity in WT-Notch1 was significantly inhibited by miR-146b-5p mimics, while miR-146b-5p did not affect the luciferase activity in MUT-Notch1 (Fig. 2B). To sum up, Notch1 was identified to be the downstream mRNA of miR-146b-5p.

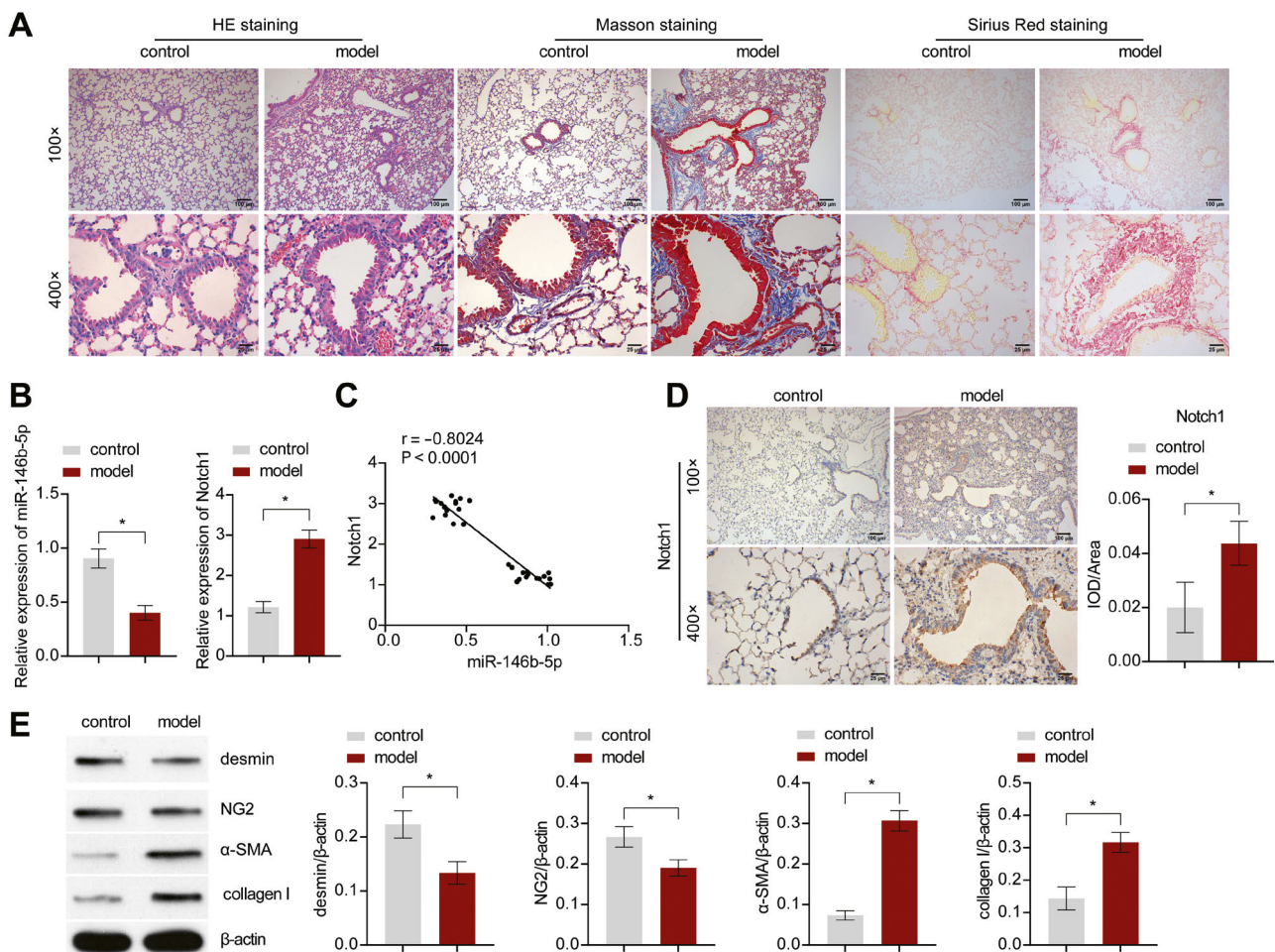


Fig. 1. *In vivo* model of lung fibrosis was successfully established. **(A)** The injury and fibrosis in lung tissues of mice were investigated by HE, Masson and Sirius Red staining, respectively. **(B)** The expression of miR-146b-5p and Notch1 in lung tissues of mice was assessed by RT-qPCR. **(C)** The correlation between miR-146b-5p and Notch1 was analysed by Spearman analysis. **(D)** The expression of Notch1 in lung tissues of mice was assessed by IHC staining. **(E)** The protein levels of desmin, collagen I, NG2 and α -SMA in lung tissues of mice were assessed by Western blot. β -Actin was applied for normalization. * $P < 0.05$.

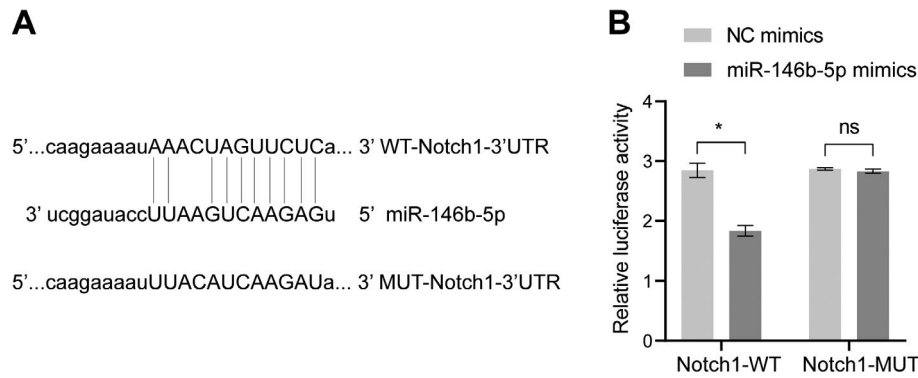


Fig. 2. Notch1 was identified to be the downstream mRNA of miR-146b-5p. (A) TargetScan was used to predict the downstream mRNAs of miR-146b-5p. (B) The relative luciferase activity in WT/MUT-Notch1 was assessed by dual luciferase assay. * $P < 0.05$.

MiR-146b-5p up-regulation inhibited proliferation of pericytes in mice with lung fibrosis

To investigate the function of miR-146b-5p in lung fibrosis, pericytes were isolated from lung tissues of mice with lung fibrosis. Then, cells were identified by immunofluorescence staining. As demonstrated in Fig. 3A, CD13 and PDGFR β were highly expressed in the cells, and these phenomena revealed that pericytes were successfully isolated from the lung tissues of mice with lung fibrosis. Meanwhile, the miR-146b-5p mimics significantly up-regulated the expression of miR-146b-5p in the tissues of mice (Fig. 3B). In contrast, the viability of pericytes was significantly decreased by up-regulation of miR-146b-5p (Fig. 3C). Consistently, miR-146b-5p mimics greatly induced G1 arrest and decreased the percentages of S and G2 phase distributions in the pericytes (Fig. 3D). Furthermore, miR-146b-5p up-regulation obviously increased the level of NG2 and inhibited the expression of α -SMA in the pericytes of mice with lung fibrosis (Fig. 3E). Taken together, miR-146b-5p up-regulation inhibited proliferation of pericytes in the mice with lung fibrosis.

Up-regulation of miR-146b-5p inhibited the fibrosis in pericytes through inactivation of the Notch1/PDGFR β /ROCK1 pathway

In order to explore the mechanism by which miR-146b-5p mimics regulated the progression of lung fibrosis, RT-qPCR and Western blot were performed. As illustrated in Fig. 4A and 4B, the levels of Notch1, PDGFR β and ROCK1 in the pericytes of mice with lung fibrosis were markedly down-regulated by miR-146b-5p mimics. Thus, it could be suggested that up-regulation of miR-146b-5p inhibited the fibrosis in pericytes through inactivation of the Notch1/PDGFR β /ROCK1 pathway.

MiR-146b-5p up-regulation modulated the fibrotic proteins in pericytes of mice with lung fibrosis

To further investigate the function of miR-146b-5p in fibrosis-related proteins, RT-qPCR and Western blot were used. The data showed that up-regulation of miR-146b-5p significantly increased the levels of desmin, NG2 and inhibited the expression of α -SMA and collagen I in pericytes (Fig. 5A and 5B). All these results indicated that miR-146b-5p up-regulation modulated the fibrotic proteins in pericytes of mice with lung fibrosis.

Discussion

It has been indicated that miR-146b-5p could alleviate tissue fibrosis. For example, miR-146b-5p is down-regulated in fibroblasts from patients with IPF (Mullenbrock et al., 2018); miR-146b-5p is involved in the alveolar and myocardial hypoxia-induced fibrosis and cardiac dysfunction, which might contribute to heart failure (Chouvarine et al., 2019). In the present research, miR-146b-5p was found to be down-regulated in lung fibrosis, and miR-146b-5p up-regulation inhibited proliferation of pericytes of mice with lung fibrosis. Notch1 is a recognized key mediator in tumour progression and inflammatory responses (Gharaibeh et al., 2020; Lee et al., 2020). In addition, Notch1 could be involved in the progression of tissue fibrosis as activation of the Notch1 pathway leads to the development of fibrosis (Lu et al., 2021; Xu et al., 2021). Therefore, our research firstly explored the relation between miR-146b-5p and Notch1 in the lung fibrosis. Our study revealed Notch1 as the downstream target of miR-146b-5p. Consistently with the previous reports exploring the role of Notch in development of tissue fibrosis, our study revealed that Notch1 was up-regulated in experimental lung fibrosis, and miR-146b-5p up-regulation inhibited the expression of Notch1 in mice with lung fibrosis.

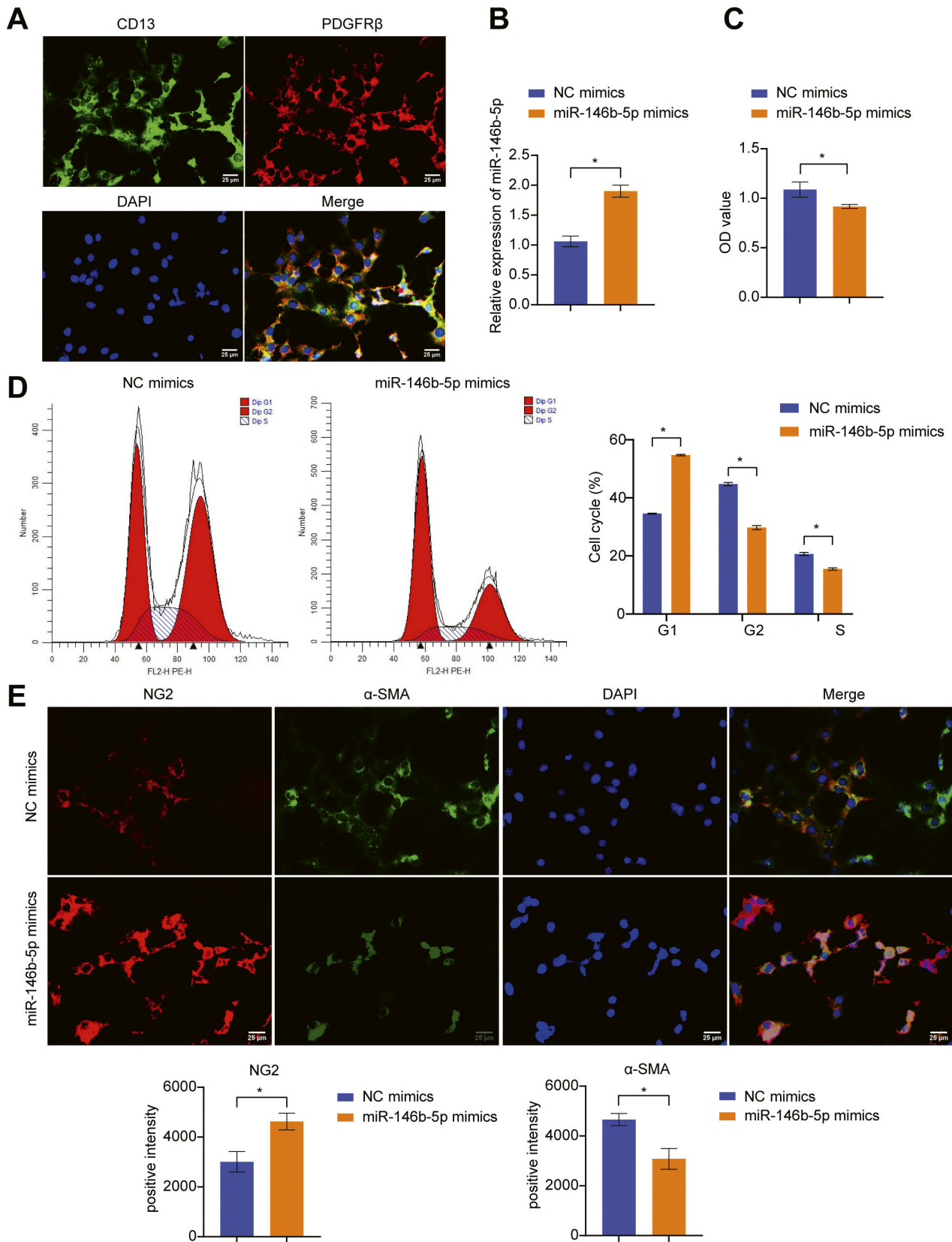


Fig. 3. MiR-146b-5p up-regulation inhibited proliferation of pericytes in mice with lung fibrosis. **(A)** Pericytes were identified by CD13 and PDGFR β staining. **(B)** Pericytes were transfected with NC mimics or miR-146b-5p mimics. The level of miR-146b-5p in the pericytes was assessed by RT-qPCR. **(C)** The viability of pericytes was assessed by CCK8 assay. **(D)** The cell cycle distribution was assessed by flow cytometry. **(E)** The expression of α -SMA and NG2 in the pericytes was evaluated by immunofluorescence staining. * $P < 0.05$.

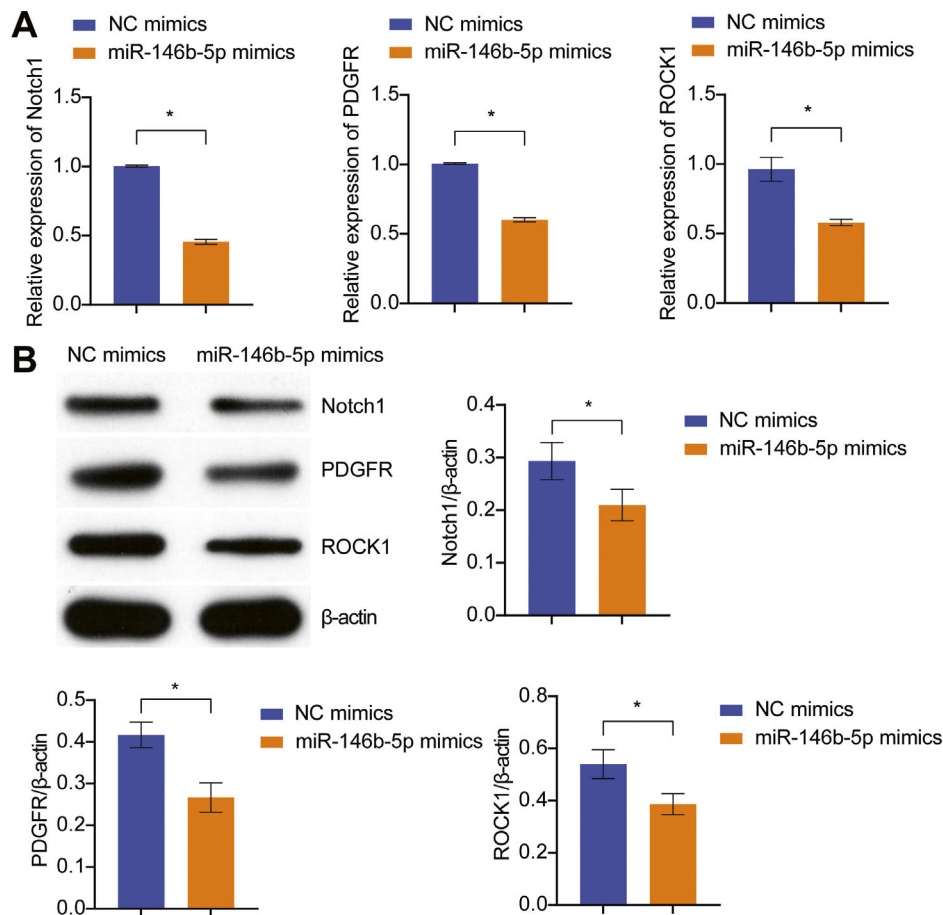


Fig. 4. Up-regulation of miR-146b-5p inhibited the fibrosis in pericytes through inactivation of the Notch1/PDGFR β /ROCK1 pathway. **(A)** The mRNA levels of Notch1, PDGFR β and ROCK1 in the pericytes of mice with lung fibrosis were investigated by RT-qPCR. **(B)** The protein levels of Notch1, PDGFR β and ROCK1 in the pericytes of mice with lung fibrosis were assessed by Western blot. * $P < 0.05$.

PDGFR β and ROCK1 are known downstream proteins of Notch1 (Wang et al., 2019). Wang et al. (2019) showed that Notch1 promotes the pericyte-myofibroblast transition in idiopathic pulmonary fibrosis through the PDGFR/ROCK1 signal pathway. We hypothesized that miR-146b-5p could inhibit the Notch1/PDGFR β /ROCK1 pathway and production of fibrotic proteins. The present study demonstrated that miR-146b-5p could inactivate the Notch1/PDGFR/ROCK1 signalling during the development of experimental lung fibrosis and modulate the fibrotic activity of pericytes. Relevant to this might be the finding that PDGFR β is involved in the transition of pericytes into glioma cells in the brain of mice (Svensson et al., 2015). Downstream proteins of PDGFR β include PI3K, Ras, PLC and ROCK1. Among these proteins, ROCK1 was suggested to play a role in lung fibrosis (Knipe et al., 2018; Yan et al., 2021; Li et al., 2022). In the present study, we demonstrated that ROCK1 was involved in the Notch1-mediated pericyte function, suggesting that ROCK1 might act as a key factor in the development of lung fibrosis. Previous evidence has shown that different pericyte subsets respond

differently to experimental tissue fibrosis (Birbrair et al., 2014). Only type-1 pericytes, but not type-2 pericytes, were involved in the lung fibrosis (Birbrair et al., 2014). In our study, we did not discriminate between the pericyte subsets.

In summary, our research explored the involvement of miR-146b-5p in the development of lung fibrosis as well as the mechanism underlying the anti-fibrotic function of miR-146b-5p. It has shown that up-regulation of miR-146b-5p inhibits the fibrotic activity of lung pericytes via the Notch1/PDGFR β /ROCK1 pathway. Thus, our findings suggest novel therapeutic targets aimed at development of lung fibrosis.

Conflicts of interest

The authors declare that they have no conflicts of interest.

Ethics approval

This study was approved by the Ethics Committee of the Hunan Provincial People's Hospital (2022-92). All experimental procedures were conducted in accordance

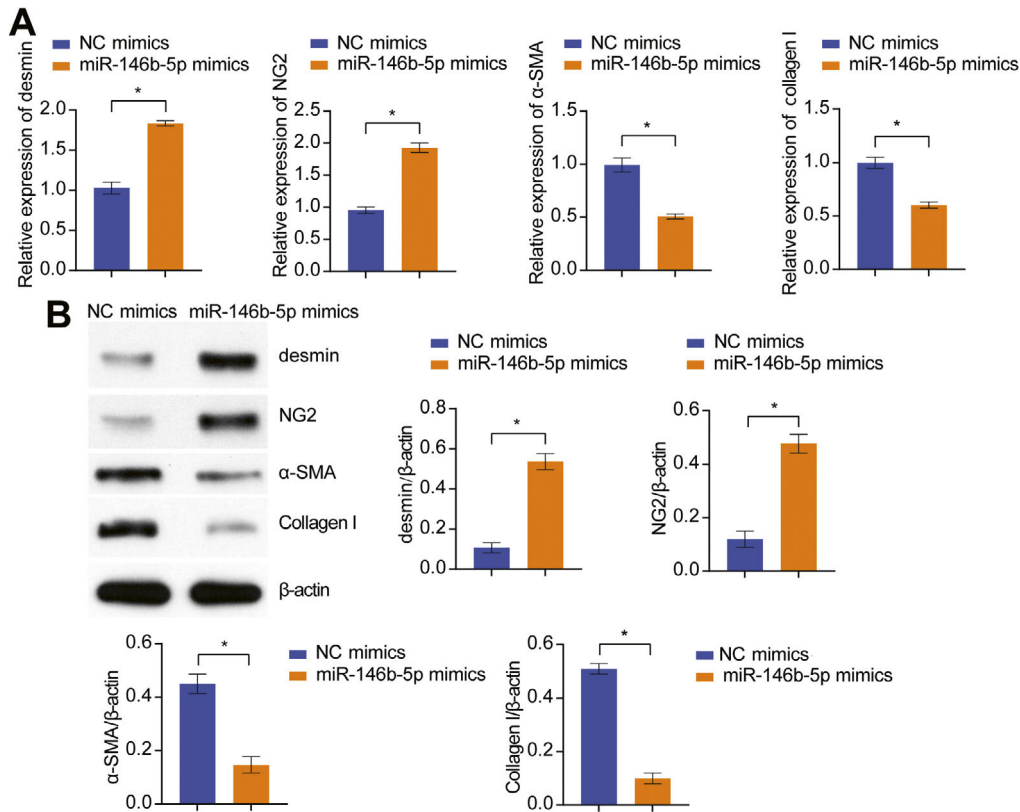


Fig. 5. MiR-146b-5p up-regulation regulated the fibrotic proteins in pericytes of mice with lung fibrosis. **(A)** The mRNA levels of desmin, collagen I, NG2 and α -SMA in the pericytes of mice with lung fibrosis were investigated by RT-qPCR. **(B)** The protein levels of desmin, collagen I, NG2 and α -SMA in the pericytes of mice with lung fibrosis were assessed by Western blot. * $P < 0.05$.

with institutional guidelines for the use of experimental animals.

Data availability

The data used to support the findings of this study are available from the corresponding author upon request.

Authors' contributions

Wei Shuai, Xu Zhou and Qiong Chen designed the study, performed the research, analysed data, and wrote the paper. All authors contributed to the article and approved the submitted version.

References

- Affandi, A. J., Carvalheiro, T., Ottria, A., de Haan, J. J., Brans, M. A. D., Brandt, M. M., Tieland, R. G., Lopes, A. P., Fernandez, B. M., Bekker, C. P. J., Van der Linden, M., Zimmermann, M., Giovannone, B., Wichers, C. G. K., Garcia, S., de Kok, M., Stifano, G., Xu, Y. J., Kowalska, M. A., Waasdorp, M., Cheng, C., Gibbs, S., de Jager, S. C. A., Van Roon, J. A. G., Radstake, T., Marut, W. (2022) CXCL4 drives fibrosis by promoting several key cellular and molecular processes. *Cell. Rep.* **38**, 110189.
- Birbrair, A., Zhang, T., Files, D. C., Mannava, S., Smith, T., Wang, Z. M., Messi, M. L., Mintz, A., Delbono, O. (2014) Type-1 pericytes accumulate after tissue injury and produce collagen in an organ-dependent manner. *Stem Cell Res. Ther.* **5**, 122.
- Chanda, D., Otoupalova, E., Smith, S. R., Volckaert, T., De Langhe, S. P., Thannickal, V. J. (2019) Developmental pathways in the pathogenesis of lung fibrosis. *Mol. Aspects Med.* **65**, 56-69.
- Chouvarine, P., Legchenko, E., Geldner, J., Riehle, C., Hansmann, G. (2019) Hypoxia drives cardiac miRNAs and inflammation in the right and left ventricle. *J. Mol. Med. (Berl.)* **97**, 1427-1438.
- Gharaibeh, L., Elmadany, N., Alwosaibai, K., Alshaer, W. (2020) Notch1 in cancer therapy: possible clinical implications and challenges. *Mol. Pharmacol.* **98**, 559-576.
- Hung, C. F., Wilson, C. L., Schnapp, L. M. (2019) Pericytes in the lung. *Adv. Exp. Med. Biol.* **1122**, 41-58.
- Ioannes, A., Morzadec, C., Duclos, M., Gutierrez, F. L., Chiforeanu, D. C., Naoures, C. L., Latour, B. D., Rouz e, S., Wollin, L., Jouneau, S., Vernhet, L. (2022) Arsenic trioxide inhibits the functions of lung fibroblasts derived from patients with idiopathic pulmonary fibrosis. *Toxicol. Appl. Pharmacol.* **441**, 115972.
- Karman, J., Wang, J., Bodea, C., Cao, S., Levesque, M. C. (2021) Lung gene expression and single cell analyses reveal two subsets of idiopathic pulmonary fibrosis (IPF) patients associated with different pathogenic mechanisms. *PLoS One* **16**, e0248889.

- Knipe, R. S., Probst, C. K., Lagares, D., Franklin, A., Spinney, J. J., Brazee, P. L., Grasberger, P., Zhang, L., Black, K. E., Sakai, N., Shea, B. S., Liao, J. K., Medoff, B. D., Tager, A. M. (2018) The Rho kinase isoforms ROCK1 and ROCK2 each contribute to the development of experimental pulmonary fibrosis. *Am. J. Respir. Cell. Mol. Biol.* **58**, 471-481.
- Lee, S., Kim, S. K., Park, H., Lee, Y. J., Park, S. H., Lee, K. J., Lee, D. G., Kang, H., Kim, J. E. (2020) Contribution of autophagy-Notch1-mediated NLRP3 inflammasome activation to chronic inflammation and fibrosis in keloid fibroblasts. *Int. J. Mol. Sci.* **21**, 8050.
- Li, Q., Cheng, Y., Zhang, Z., Bi, Z., Ma, X., Wei, Y., Wei, X. (2022) Inhibition of ROCK ameliorates pulmonary fibrosis by suppressing M2 macrophage polarisation through phosphorylation of STAT3. *Clin. Transl. Med.* **12**, e1036.
- Lu, L., Ma, J., Liu, Y., Shao, Y., Xiong, X., Duan, W., Gao, E., Yang, Q., Chen, S., Yang, J., Ren, J., Zheng, Q., Liu, J. (2021) FSTL1-USP10-Notch1 signaling axis protects against cardiac dysfunction through inhibition of myocardial fibrosis in diabetic mice. *Front. Cell. Dev. Biol.* **9**, 757068.
- Maher, T. M., Streck, M. E. (2019) Antifibrotic therapy for idiopathic pulmonary fibrosis: time to treat. *Respir. Res.* **20**, 205.
- Mullenbrock, S., Liu, F., Szak, S., Hronowski, X., Gao, B., Juhasz, P., Sun, C., Liu, M., McLaughlin, H., Xiao, Q., Feghali-Bostwick, C., Zheng, T. S. (2018) Systems analysis of transcriptomic and proteomic profiles identifies novel regulation of fibrotic programs by miRNAs in pulmonary fibrosis fibroblasts. *Genes (Basel)* **9**, 588.
- Svensson, A., Ozen, I., Genove, G., Paul, G., Bengzon, J. (2015) Endogenous brain pericytes are widely activated and contribute to mouse glioma microvasculature. *PLoS One* **10**, e0123553.
- Wang, Y. C., Chen, Q., Luo, J. M., Nie, J., Meng, Q. H., Shuai, W., Xie, H., Xia, J. M., Wang, H. (2019) Notch1 promotes the pericyte-myofibroblast transition in idiopathic pulmonary fibrosis through the PDGFR/ROCK1 signal pathway. *Exp. Mol. Med.* **51**, 1-11.
- Wang, Y. C., Liu, J. S., Tang, H. K., Nie, J., Zhu, J. X., Wen, L. L., Guo, Q. L. (2016) miR221 targets HMGA2 to inhibit bleomycin-induced pulmonary fibrosis by regulating TGFbeta1/Smad3-induced EMT. *Int. J. Mol. Med.* **38**, 1208-1216.
- Wang, Y. C., Xie, H., Zhang, Y. C., Meng, Q. H., Xiong, M. M., Jia, M. W., Peng, F., Tang, D. L. (2021) Exosomal miR-107 antagonizes profibrotic phenotypes of pericytes by targeting a pathway involving HIF-1 α /Notch1/PDGFRbeta/YAP1/Twist1 axis in vitro. *Am. J. Physiol. Heart Circ. Physiol.* **320**, H520-H534.
- Xu, Q. X., Zhang, W. Q., Liu, X. Z., Yan, W. K., Lu, L., Song, S. S., Wei, S. W., Liu, Y. N., Kang, J. W., Su, R. W. (2021) Notch1 signaling enhances collagen expression and fibrosis in mouse uterus. *Biofactors* **47**, 852-864.
- Yan, J., Tang, Y., Zhong, X., Huang, H., Wei, H., Jin, Y., He, Y., Cao, J., Jin, L., Hu, B. (2021) ROCK inhibitor attenuates carbon blacks-induced pulmonary fibrosis in mice via Rho/ROCK/NF-kappa B pathway. *Environ. Toxicol.* **36**, 1476-1484.
- Yu, S., Li, L., Tian, W., Nie, D., Mu, W., Qiu, F., Liu, Y., Liu, X., Wang, X., Du, Z., Chu, W. F., Yang, B. (2018) PEP06 polypeptide 30 exerts antitumour effect in colorectal carcinoma via inhibiting epithelial-mesenchymal transition. *Br. J. Pharmacol.* **175**, 3111-3130.